Harmonic millimeter radiation from a microwave free-electron-laser amplifier

Y-H. Liu and T. C. Marshall
Department of Applied Physics, Columbia University, New York, New York 10027
(Received 20 January 1997)

Using a free-electron laser (FEL) configured as a traveling-wave amplifier, we have caused the bunching produced by the amplification of a coherent microwave source to drive appreciable power at the harmonics. A 10-kW 24-GHz microwave input signal grows to the ~200 kW level using the lower frequency unstable root of the waveguide FEL dispersion relation. The FEL operates in the TE11 mode, using a helical undulator (1.85-cm period) and a 3-mm-diam 600-kV electron beam contained in an 8.7-mm-i.d. cylindrical waveguide. The harmonic currents set up by the microwave are found to cause growth of harmonic power under two conditions. First, if the design is such that the upper frequency root corresponds to the third harmonic, we see small amounts of third- and second-harmonic power, coherent with the source. Second, we have found kW emission of the seventh harmonic, most likely from the TE72 mode, which travels at the same speed as the 24-GHz wave. In order to excite the seventh-harmonic radiation, the electron beam must be displaced from the axis of the guide by ~2 mm. In both cases, no harmonic power is produced without gain at the fundamental. We present a one-dimensional theoretical model of the experiment, and use the numerical results to interpret our findings. The model predicts that if the microwave signal is strong enough to drive the FEL into saturation, the harmonic radiation should become powerful. [S1063-651X(97)14108-3]

PACS number(s): 41.60.Cr

INTRODUCTION

If an electron beam undergoing FEL (free-electron laser) interaction is bunched by a coherent source of power, then FEL harmonic radiation will grow from an initial condition that is very much above noise input. The radiation at the harmonics should be related in phase and frequency to the source, which bunches the electron beam. However, lacking some resonant or phase-matching process, typically harmonic radiation remains at a low level [1]. Appreciable harmonic power depends on gain at the FEL harmonic [2], or on some mechanism to couple energy from the lower frequency FEL wave into the harmonic. In this paper we study an example of each of these.

Recently, Piovella *et al.* [3] studied a waveguide FEL where the beam is bunched by a growing wave at the low frequency beam-wave intersection, prompting growth at a harmonically related high frequency upper intersection [see Eq. (1) below]; a similar idea was described by Sternbach and Ghalila [4]. In the waveguide FEL, there are two unstable roots of the dispersion relation that represent, in the work we describe in this paper, growing TE11 waves at 24 and ~72 GHz (third harmonic); the frequencies are obtained approximately by calculating the intersections between the beam wave dispersion and the electromagnetic wave dispersion curves in a waveguide, neglecting the Raman space charge effect:

$$\omega_{1,2}=\frac{\omega_s}{1+\beta}\left[1\pm\beta\sqrt{1-X}\right], \tag{1}$$

where $\omega_s=c\beta k_w/(1-\beta)$ and $k_w=2\pi/l_w$. X involves the cutoff frequency of the waveguide, $X=[(1.84/2\pi R_g)l_w/\beta\gamma_\parallel]^2$. Here, $\beta c=v_\parallel$ the axial electron velocity, $\gamma_\parallel$ is the corresponding relativistic factor, l_w is the undulator period, R_g is the cylindrical waveguide radius, and c is the speed of light. Thus one might generate frequency and phase stable millimeter power in a FEL amplifier using a microwave source for bunching; and because the high frequency harmonic wave in the FEL is also growing, the power output in principle can be high. We have reported already on an experiment that studies such harmonic radiation from a FEL—configured as a traveling-wave amplifier—using a magnetron source to drive the low frequency FEL mode [5].

In this paper, we give further data and interpretation regarding the experimental properties of this interaction. Also, our recent observation [6] of appreciable *seventh*-harmonic power is a potentially significant development, and involves a mechanism that is different [7] from that described above; we shall present experimental results and interpretation of this effect as well. In the following, we present a theory and a numerical simulation of the experiments that makes use of the FEL equations using two waves, harmonically related in frequency but traveling at different speeds in a waveguide.

EXPERIMENT

Figure 1 shows a schematic of the FEL apparatus, which is driven by a pulseline generator [8]. This pulseline produces a 150-nsec, nearly flat voltage pulse (400–600 kV),

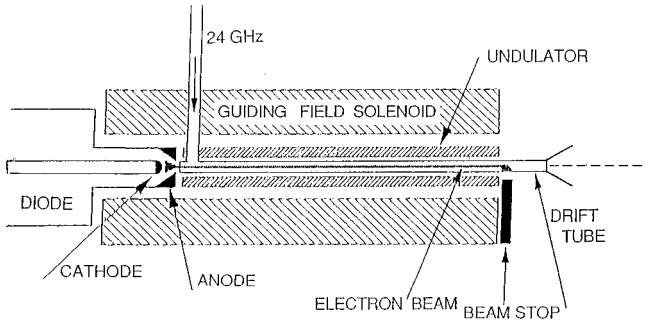

FIG. 1. Schematic: a pulseline source provides a negative 150-nsec pulse to a graphite diode that ''apertures'' the electron beam.

TABLE I. Parameters of the FEL.

	Col. 1	Col. 2
Electron energy	600 kV	
Low frequency FEL mode	24 GHz	
High frequency FEL mode	72 GHz	
Undulator period	2.5 cm	1.85 cm
aw, effective undulator parameter	0.2	
Guide field	0 G	8800 G
TE11 cutoff frequency	18.4 GHz	20.7 GHz
Electron beam current	~100 A	
Electron beam diam	~3 mm	

which is applied to a cold graphite cathode in a field-immersed vacuum diode. The solenoidal field is primarily for beam transport, but it also slightly enhances the spiraling motion of the electrons moving through the undulator (quiver velocity $\sim 0.1c$). The electron current emitted from the cathode is ''apertured'' by a 3-mm-diam hole in a graphite anode to improve the beam quality; the beam carries about 100 A. Table I lists parameters of the device appropriate to the experiment, which is conducted in the ''Raman'' regime (column 2), whereas the first column refers to equivalent parameters for the ''Compton'' theory. A 24-GHz 10-kW signal obtained from a magnetron is launched in the TE11 mode inside a cylindrical stainless steel waveguide, enclosed by a helical undulator. A relatively small value of undulator field (~250 G) is chosen so that the system behaves like a traveling-wave amplifier with a gain <50, in which case oscillation is avoided; also, numerical study of the electron motion has shown that a low undulator field will give stable well-behaved electron orbits in the combined undulator and guide fields. The propagation and alignment of the electron beam through the waveguide were studied by taking a series of ''witness plates.'' (The latter determines the beam location via a damage pattern on a piece of thermal-sensitive paper.) The diameter of the waveguide and undulator period are chosen so that there is exponential gain of the 24-GHz wave and one of the harmonics at an electron beam energy of 600 kV; a single frequency code [9] that includes the one-dimensional (1D) motion and the 2D wave equations in the cylindrical waveguide was used for this design. Figure 2 shows the computed gain [9] of the device for beam energies of 600 and 400 kV, taking the fundamental and harmonic waves to be in the TE11 mode.

Using a grating spectrometer adapted for millimeter-wave studies [10], we have found 24-GHz power gain ~20 (well below saturation), and the observation of the first three harmonics (~100 W, peak) has been reported [5]. No harmonic power is obtained unless there is appreciable gain for the 24-GHz wave (compare corresponding traces, Fig. 3). The third-harmonic power output was found to be greater than the second, and both are much greater than the fourth (Fig. 4) or higher harmonics. If the interaction were nonresonant, then the power of the harmonics should fall off very rapidly [1] with increasing harmonic number. The power gain at 72 and 48 GHz for the operating condition of beam voltage of 600 kV should be about 10, according to Fig. 2; this figure shows the gain maxima that result from the two intersections described by Eq. (1). Figure 3 shows the result (lower trace)

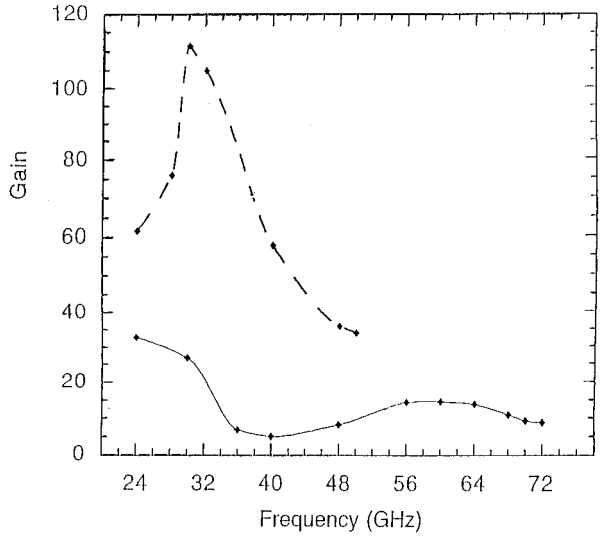

FIG. 2. Computed FEL gain vs frequency, for parameters of Table I, column 2, for beam energy of 600 kV (solid line) and 400 kV (dashed line).

of mixing the 72-GHz FEL third-harmonic signal with the frequency tripled magnetron signal, demonstrating a fixed frequency relationship between the FEL third-harmonic power pulse and the lower frequency magnetron power that drives the FEL bunching.

We have also observed the emission of appreciable seventh-harmonic power, 168 GHz (spectrum, Fig. 4), obtained only when we have appreciable gain for the 24-GHz FEL wave and when there was a misalignment of our system in which the electron beam was moved about 2 mm off the waveguide axis. The seventh-harmonic signal level is ~1 kW or more, whereas the 24-GHz signal is amplified to ~200 kW, much less than saturation. The seventh harmonic is not a ''resonant FEL interaction'' and its appearance should depend on two special conditions. The first is that the

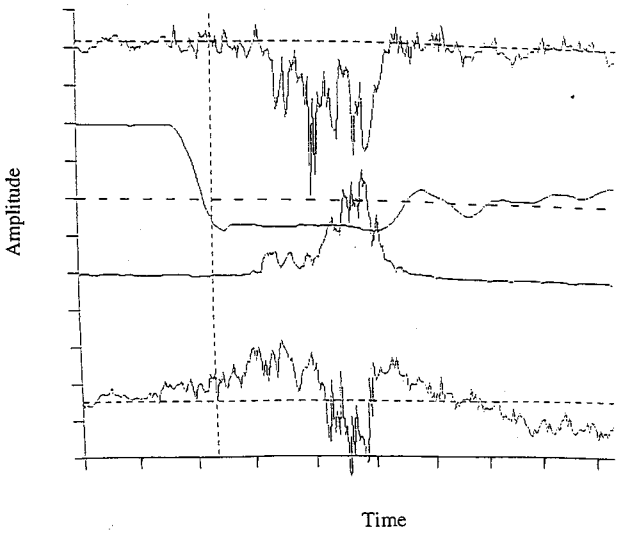

FIG. 3. From below: beat signal envelope of FEL third harmonic mixed with magnetron tripled frequency; 24-GHz amplified signal; diode voltage of accelerator (~600 kV); 72 GHz detector signal. Horizontal scale: 50 nsec/div; diode voltage vertical scale: 200 kV/div.

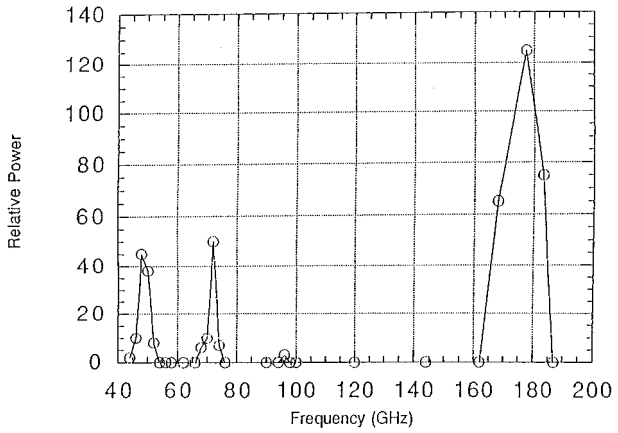

FIG. 4. Power spectrum scan, covering harmonics 2–8; beam is off axis for harmonics >5 (signals for the seventh harmonic and harmonics >5 are zero for on-axis beam). Data points represent average of several shots, recording peak power.

temporal and spatial spectrum of the seventh-harmonic electromagnetic wave must move at very nearly the same wave velocity as the temporal and spatial spectrum of its electron current source, the latter being set up by the seventh temporal harmonic of the bunching caused by the amplified TE11 24-GHz wave. The EM wave in question that satisfies this constraint is the TE72 mode of the cylindrical waveguide [7], since this wave has the same wave refractive index as the TE11 wave at 24 GHz. Also, this mode has zero field on axis, and therefore the electron beam must be moved off axis to overlap one of the electric field maxima of the TE72 wave. We have observed the seventh-harmonic signal in this device for an electron beam energy of 600 kV and as low as 400 kV (Fig. 5), since there is gain at 24 GHz at the lower energy (see Fig. 2).

In contrast to the ''second-order'' FEL resonant wave interaction (which commences from zero source current and field, apart from noise, but grows exponentially), the harmonic conversion is a ''first-order'' process [11], in which the beam is already prepared so that its equilibrium current carries spatiotemporal modulation at the harmonic (this

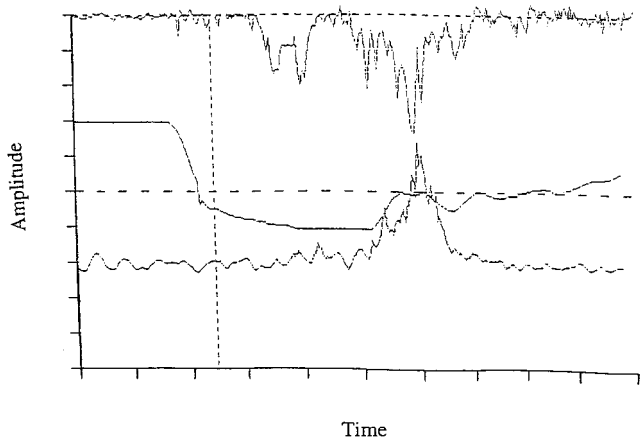

FIG. 5. 24-GHz amplified power (below) and 168-GHz converted power (above), obtained when the diode voltage (middle) is only about 400 kV; similar result can be obtained at 600 kV as well. Same scale axes as Fig. 3.

modulation is set up by the FEL resonant interaction at 24 GHz). Thus there is no need for a ''linearized dispersion relation'' for the first-order conversion. What must happen, however, is that the wave that feeds on the seventh-harmonic currents in the beam must travel at the same speed as these currents if there is to be efficient conversion. The FEL interaction, which generates a wide spectrum of harmonics as the beam becomes progressively more bunched, is the free energy source for the seventh harmonic.

THEORY

To study the coupling between the harmonically related waves, we solve numerically the set of FEL equations with slippage for the electron dynamics and two interacting waves [5]. For simplicity, we disregard the space-charge (Raman effect), which will decrease the gain and require a shorter undulator period to provide the same frequencies as used in this calculation. The parameters of the calculation are given in Table I, column 1. The low-frequency (24 GHz) TE11 FEL mode has group velocity $\sim c/2$, as does the seventh-harmonic TE72 wave; the second- and third-harmonic TE11 FEL wave group velocities are higher than the electron speed $(\sim 0.88c)$.

We first define the variables x and y as

$$x = A\left[t - \frac{z}{v_{g2}}\right], \quad y = A\left[\frac{z}{v_{\parallel}} - t\right],$$

where $A = [1_w(1/v_{\parallel} - 1/v_{g2})]^{-1}$ and v_{g1}, v_{g2} are the group velocities of ω_1 and ω_2, $v_{\parallel}$ is the electron axial speed, and z,t are the axis and time variables. Defining a_1 and a_2 ($a_1 = a_{s1}e^{-i\phi_1}$) as the normalized vector potentials of waves 1 and 2, which have axial wave numbers k_1 and k_2 in the waveguide, respectively, and a_w the undulator potential $eB_w l_w/2\pi mc^2$, where B_w is the undulator field, the electron and wave equations for the jth electron are

$$\frac{\partial \theta_{2j}}{\partial x} = l_w \overline{k_{w2}}\left(1 - \frac{\overline{\gamma_{r2}^2}}{\gamma_j^2}\right), \tag{2}$$

$$\frac{\partial \gamma_j}{\partial x} = -1_w \frac{a_w}{\gamma_j v_{\parallel j}} [\omega_1 a_{s1} \sin(\alpha\theta_{2j} + \phi_{1j}) + \omega_2 a_{s2} \sin(\theta_{2j} + \phi_{2j})], \tag{3}$$

$$\left\{\frac{\partial}{\partial y} + \left(\frac{1/v_{g1} - 1/v_{g2}}{1/v_{\parallel} - 1/v_{g1}}\right)\frac{\partial}{\partial x}\right\} a_1 = \frac{i}{A(1/v_{\parallel} - 1/v_{g1})} \frac{\omega_p^2 a_w}{2c^2 k_1} \left\langle \frac{e^{-i\alpha\theta_2}}{\gamma} \right\rangle, \tag{4}$$

$$\frac{\partial a_2}{\partial y} = i l_w \frac{\omega_p^2 a_w}{2c^2 k_2} \left\langle \frac{e^{-i\theta_2}}{\gamma} \right\rangle. \tag{5}$$

These equations also involve the following quantities: ω_p, the beam plasma frequency; α, the harmonic number; $\theta_2 = k_w z + k_2 z - \omega_2 t$; $\phi_{1,2}$, the optical phase; and

$$\overline{k_{w2}} \equiv k_w + k_2 - \omega_2/c, \quad \overline{\gamma_{r2}^2} \equiv k_2(1 + a_w^2)/2\overline{k_{w2}}.$$

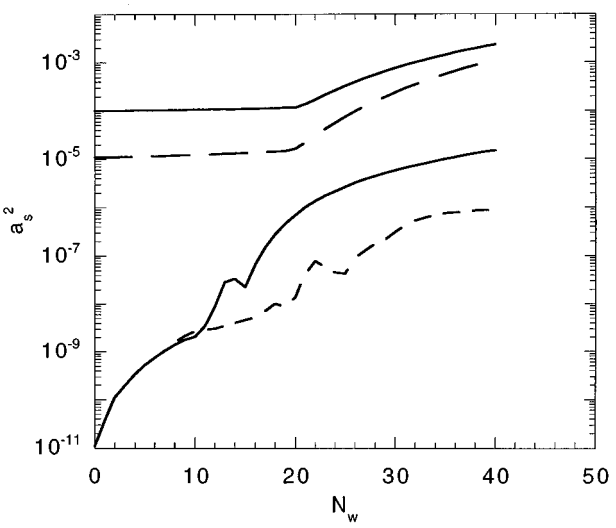

FIG. 6. 24-GHz FEL power growth (line pair above) and 168-GHz power converted (line pair below) in units of normalized wave vector potential squared, vs axial distance measured in undulator periods. There is a 1% mismatch of wave group velocity, and two cases are shown: for initial 24-GHz microwave power of 10 kW (broken lines) and 100 kW (solid lines).

In the simulation, the FEL behaves as a traveling-wave amplifier. The spatial distribution of simulation electrons has a rectangular profile, the electrons are taken to be monoenergetic, and at the undulator entrance $z=0$ they are uniformly distributed inside the beam length with 100 simulation electrons per undulator period. For each wavelength-size strip of particles, the relative phase location of the electrons with respect to the radiation field is uniformly distributed between $-\pi$ and π. For the output format of the computational results, the electron beam pulse and the radiation pulse (each taken to be flat-topped) are plotted as a function of the variables x and y, which imply two moving ''windows,'' the former at v_{g2} and the latter at $v_{\|}$; both are scaled in units of the undulator period. The electron motion is parallel to the x axis while the ω_2 wave moves parallel to the y axis; the ω_1 wave moves along the characteristic

$$x-\left(\frac{1}{v_{g1}}-\frac{1}{v_{g2}}\right)\left(\frac{1}{v_{\|}}-\frac{1}{v_{g1}}\right)^{-1}y=\text{const.}$$

The finite radial size of the electron beam is accounted for in the code using a multiplicative ''filling factor'' for the radiation current term on the right-hand sides of Eqs. (4) and (5). While this can be estimated from geometry, it is also a convenient parameter to adjust the gain of the 24-GHz wave so that it corresponds to our observations.

Figure 6 is an example we calculated that is relevant to the seventh-harmonic experiment. It shows the peak power growth along the undulator of the 24- and 168-GHz waves starting from an initial signal of 10 kW at 24 GHz in the right circular ''rotating'' mode; the two waves travel at nearly the same speed (the group velocity is about $0.5c$ in the waveguide). The figure shows that the conversion of microwave power to the seventh harmonic is $\sim 7\%$ when the signal reaches the end of our undulator, ~ 32 periods. This calculation (broken line pair) is for a wave speed mismatch

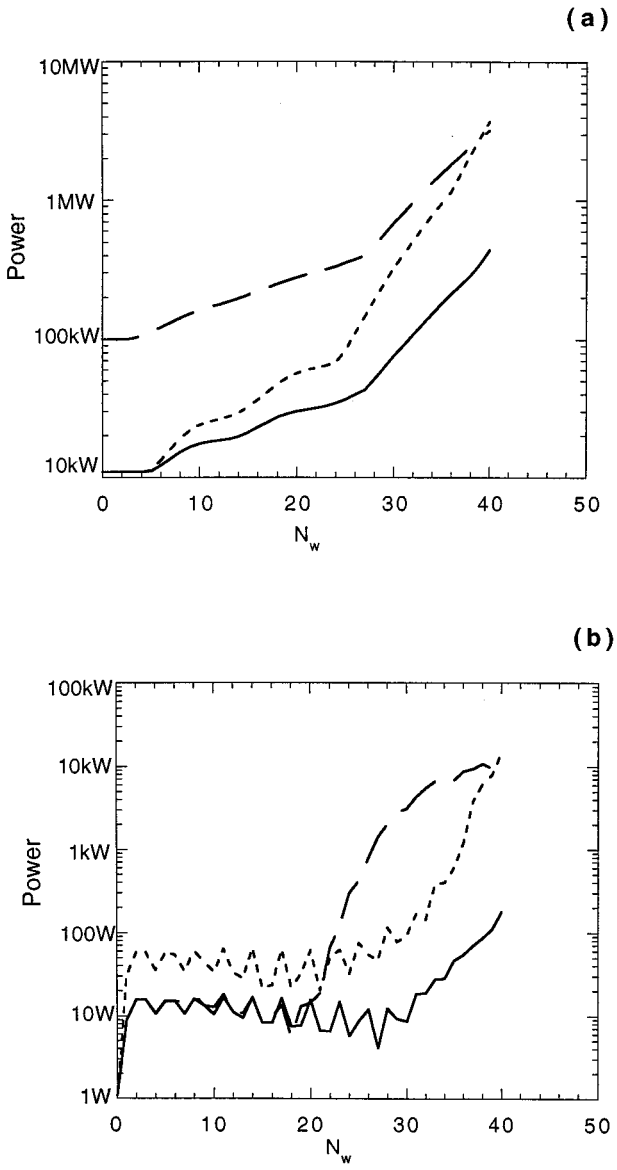

FIG. 7. Power growth of 24 (a), and 72 GHz (b) waves vs axial distance measured in undulator periods. The three examples are as follows. Solid line: initial microwave power 10 kW and gain of 40; dashed line: initial microwave power 100 kW and gain of 40; dotted line: initial microwave power 10 kW and gain of 400. The first case is that of the experiment where ~ 100 W at 72 GHz is produced; in the other examples, the 72-GHz power level is ~ 10 kW at 40 undulator periods. The gain of the 24 GHz wave is varied by changing the beam filling factor: 0.2 for low gain (experimental), and 0.35 for the higher gain example.

(between the 24- and the 168-GHz signals) of 1%, approximately what is expected from the theory [7]. However, if the FEL output is driven near saturation (~ 2 MW, solid line pair), the computation reveals that the seventh-harmonic power becomes nearly 30% of the microwave power. We point out that this is a 1D simulation and the overlap between the particles and the different radiation modes is being modeled with the same filling factor. Since a 3D simulation is really necessary to model the off-axis behavior of the beam and its overlap with the waveguide mode, the results of this calculation cannot be compared with the experiment quanti-

tatively, but may serve as an incentive for further study. Indeed, a 3D code [12] has been used recently to model the generation of the seventh-harmonic signal. Appreciable seventh-harmonic output (~ 2 kW) has been found [13] using the Raman version of this code with the electron beam located off axis; much smaller power (~ 200 W) was found when the beam was located on axis. These results, which are not much different from our experimental findings, will be presented in more detail elsewhere, as the optimum location of the electron beam for power conversion has yet to be found.

Figure 7 shows the increase of 24-GHz (power gain $=40$) and 72-GHz power, starting from 10 and 100 kW of the 24-GHz signal. The two waves travel, respectively, at a group velocity of $\sim c/2$, and $0.96c$. This is the ''beam-on-axis'' case, where the particles couple to the TE11 mode. The third-harmonic power reaches a level of 100 W and 10 kW, respectively. Another example is computed where the low frequency wave starts off at 10 kW, but experiences a power gain ~ 400. By comparing these examples, one finds that in order to get harmonic power of tens of kW it is necessary to have either a large input microwave power or a high-gain system: the requirement is that the device achieves a microwave power output near the saturation level so that the harmonics of the bunching are large [1]. The figure shows that the harmonic output is very sensitive to the output microwave power; we find that as much as 70 kW of third harmonic can be produced if the computation is carried further along to 50 undulator periods. The simulation, which compares with the experiment (solid line), shows the emission of only a small amount of power, as we have found. The harmonic power begins its rapid growth when the bunching produced by the microwaves develops a substantial harmonic component; until then (at $N_w < 20$), the bunching harmonic and its wave amplitude remain small and ''noisy'' [1].

CONCLUSIONS

We believe the harmonic power observed in this experiment can be of use to create coherent, phase-referenced power in the millimeter spectrum for applications such as radar and accelerator physics. The higher frequency waves are driven by the bunching set up by the microwave source, and we have shown in the example of the third harmonic that this signal has a fixed relationship to the lower frequency source. The third-harmonic radiation does not compete with the seventh for the free energy of the bunching, because the seventh harmonic does not occur when the electron beam is positioned on the axis. On the other hand, one can suppress the lower harmonics by making the FEL interaction resonant at *one* microwave frequency only [by arranging that the second term in the square brackets of Eq. (1) vanishes], together with positioning the electron beam *off*-axis to enhance the seventh-harmonic coupling. The latter approach may represent a very convenient way to generate appreciable 2-mm wavelength power, using a FEL operating at comparatively low beam energy driven by a powerful microwave source. In our experiment, due to low gain of the system (~ 13 dB) and the modest microwave power available at the FEL input, the power output of the harmonics is not high. However, the theory shows that one can expect substantial harmonic output if the FEL amplifier is operated so that the input microwave signal becomes nearly saturated at the output.

ACKNOWLEDGMENT

This research was supported by the Office of Naval Research.

[1] Y.-P. Chou and T. C. Marshall, Nucl. Instrum. Methods Phys. Res. A **318**, 528 (1992).

[2] P. G. O'Shea *et al.*, Nucl. Instrum. Methods Phys. Res. A **341**, 7 (1994).

[3] N. Piovella *et al.*, Phys. Rev. Lett. **72**, 88 (1994).

[4] E. Sternbach and H. Ghalila, Nucl. Instrum. Methods Phys. Res. A **304**, 691 (1991).

[5] Y.-H. Liu and T. C. Marshall, Nucl. Instrum. Methods Phys. Res. A **375**, 589 (1996).

[6] Y.-H. Liu and T. C. Marshall, in *Proceedings of hte 11th International Conference on High Power Particle Beams*, Prague, 1996, edited by K. Jungwirth and J. Ullschmied (Czech Academy of Sciences, Prague, 1996), Vol. I, p. 397.

[7] C. Wang, J. L. Hirshfield, and A. K. Ganguly, Phys. Rev. Lett. **77**, 3819 (1996).

[8] S. C. Chen and T. C. Marshall, IEEE J. Quantum Electron. **21**, 924 (1985).

[9] S. Y. Cai, A. Bhattacharjee, and T. C. Marshall, IEEE J. Quantum Electron. **23**, 1651 (1987).

[10] J. A. Pasour and S. P. Schlesinger, Rev. Sci. Instrum. **48**, 1355 (1977).

[11] A. K. Ganguly and J. L. Hirshfield, Phys. Rev. E **47**, 4364 (1993).

[12] H. P. Freund and T. M. Antonsen, Jr., *Principles of Free Electron Lasers* 2nd ed. (Chapman and Hall, London, 1996), Chap. 5.

[13] H. P. Freund (private communication).